Pak. j. sci. ind. res. Ser. A: phy. sci. 2023 **66A**(2) 150-161

Interaction of Magnetic Dipole with the Ferrofluid Over a Stretching Sheet

Sohail Ahmad[a]*, Kashif Ali[b] and Muhammad Ashraf[a]

[a]Centre for Advanced Studies in Pure and Applied Mathematics, Bahauddin Zakariya University, Multan 60800, Punjab, Pakistan

[b]Department of Basic Sciences and Humanities, Muhammad Nawaz Sharif University of Engineering and Technology, Multan 60000, Punjab, Pakistan

(received March 13, 2020; revised February 28, 2021; accepted March 02, 2021)

Abstract. Our concern in this article is to examine the flow and heat transportation phenomenon of viscous ferrofluid in the presence of magnetic dipole over a stretching sheet. The enforced magnetic field is supposed to be strong enough to concentrate the ferrofluid whereas the fluid magnetization is assumed to be a linear function for temperature and magnetic field intensity. The powerful tool of similarity transformation has been applied for simplification of the mathematical model and as a consequence, six parameters arise in the final model. Flow velocities as well as temperature distributions obtained under different conditions, by varying the governing parameters, are analyzed and discussed through tables and graphs. A graphical comparison is associated with the previously accomplished results and examined to be in an exceptional agreement. The culminations evidently disclose that the magnetic as well as ferrohydro dynamic parameter elevate the flow velocity. It is examined that the impact of prandtl number is to depress thermal boundary layer, while the magnetic parameter enhances the shear stress.

Keywords: ferrofluid, magnetic dipole, heat transfer, SOR

Introduction

The analysis of heat transportation and boundary layer flow past a stretching sheet has a considerable value in manufacturing and industrialization process e.g. heat exchange process, power supply in electronic devices and also in vehicle engine cooling system. Crane (1970) was a predecessor in analyzing the mechanized process related to heat transport and laminar flow of boundary layer over a stretching sheet. Afterward, numerous research scholars (Ahmad *et al*., 2020a, b, c, d & e; Ghadikolaei *et al*., 2018; Yacob and Ishak, 2012) have examined various stretching sheet problems. Besides a rich literature is available on ferrofluid flows comprising of spatially varying field over stretching sheets. Ferrofluids are synthetic fluids experiencing a magnetization force. The magnetization of ferrofluids is temperature dependent and this thermomagnetic coupling property leads the ferrofluids towards significant fluids in manufacturing and industrialization (Tangthieng *et al*., 1999; Eringen *et al*., 1990). Ferro hydrodynamics can be distinguished from magneto-hydrodynamics because of the existing of spatially varying field. It is essential to synthesize innovative fluids for bio-technology, engineering and geophysics. Ferrofluids, also known as magnetic fluids, which are significantly purposeful fluids. These fluids are chemically stable colloidal suspensions entailing the magnetic particles with a diameter ranging from 5-15 nm (Papell and Stephen, 1965). Because of this diameter size of magnetized particles, these fluids may also called magnetic nanofluids. Ferrofluids act like nanoparticles to strengthen thermal properties of fluid. Magnetic field changes the physical characteristics of ferrofluids e.g. temperature distribution. This property makes the ferrofluids much functional in various industries e.g. engineering and biomedical sciences.

The magneto-hydrodynamic phenomenon is widely used in the fields of astrophysics, engineering, geo-physics and aerospace engineering. Examples includes photochemical reactors, plasma confinement, fiber coating, transportation, magnetic drug targeting, heat exchangers, electromagnetic casting, x-rays, cooling of nuclear reactors, sensors and so forth. During the past few decades, the problems of magneto-hydrodynamic fluid flows with heat transport have been intensely studied. Recently, an analysis of MHD axisymmetric micropolar nanofluid flow through porous parallel disks was presented by Abbas *et al*. (2019) with the results

*Author for correspondence;
E-mail: sohailkhan1058@gmail.com

that the radial velocity curves rise up near the disks and diminish at the central plane. Rauf *et al*. (2019) evaluated the combined effects of Cattaneo-Christov mass and heat flux on MHD three dimensional fluid flow over an oscillatory disk. They obtained the solution of highly nonlinear ODEs with the help of finite difference discretization along with successive over relaxation (SOR) method. Shamshuddin and Thumma (2019) solved a mathematical model of MHD dissipative micropolar fluid flow through porous medium by exploiting finite element method and found that the escalating values of microrotation parameter suppress the microrotation velocity profile. Taking into account the occurrence of thermal radiation, temperature dependent slip condition and viscous dissipation in MHD two dimensional fluid flow, Gangadhar *et al*. (2017) made an effort to provide mathematical solution of the problem using bvp4c MATLAB solvers. Bhatti *et al*. (2016) deliberated the combined effects of entropy generation and thermal radiation in MHD non Newtonian fluid flow past a porous shrinking surface. They obtained the solution of highly nonlinear ODEs with the support of Chebyshev spectral collo-cation scheme along with successive linearization method (SLM). The interaction of micropolar fluid with the applied Lorentz force inside a magneto-hydrodynamic micro pump was examined by Alizadeh-Haghighi *et al*. (2017). Their results were compared with the experimental ones and found almost similar to each other for special cases.

The flows of ferrofluids have been comprehensively studied by various authors. MHD flow of cobalt-kerosene ferrofluid, under the influence of partial slip and thermal radiation, over a non-isothermal wedge was evaluated by Rashad (2017). In this research, it was found that local Nusselt number shows a remarkable reduction for magnetic parameter and enhances intensively in the presence of surface temperature and thermal radiation parameters. A mixed convective and magneto-hydrodynamic ferrofluid flow, with partial slip impacts and convective boundary conditions, over an impulsively stretchable sheet was modeled by EL-Kabeir *et al*. (2019) and El-Zahar *et al*. (2019) numerically investigated the natural convective flow of Fe_2O_4 ferrofluid over a vertical radiate plate using stream wise sinusoidal variation in surface temperature. Using finite volume method, Chamkha *et al*. (2020) studied the magneto ferrofluid mixed convection flow inside a lid driven square cavity with partial slip. The horizontal moving walls of the enclosure were kept adiabatic, while the vertical walls were heated partially by a constant temperature. The square enclosure was filled with a mixture of kerosene cobalt ferrofluids. The heat transfer rate was marginally influenced by augmentation of the ferromagnetic particles volume fraction. Nabwey *et al*. (2020) identified the characteristics of unsteady magneto-hydrodynamic (MHD) flow of ferrofluid past a radiated stretching surface.

Bognar and Hriczo, (2018) recently worked on the flow of ferrofluid under the effect of magnetic field. They examined the magneto thermo mechanical relations between a cold wall and heated viscous ferrofluid theoretically. The fully coupled equations were transformed into nonlinear coupled ones by employing similarity transformations. These ODEs were discretized into an algebraic system of equations which were then solved by means of Higher Derivative Method (HDM). Results obtained by Bognar and Hriczo, (2018) were correlated with those achieved by Neuringer (1966). Perez *et al*. (2017) examined the magnetic viscous effects on the temperature gradient by using oldroyd model. Eigen values and eigen functions were determined by solving the dynamical equations numerically using a collocation spectral method. The change between oscillatory and static inconstancy was a little bit affected by magnetic effects. Zeeshan *et al*. (2016) and Abraham *et al*. (2011) explored numerically the impact of magnetic dipole and heat source/sink on ferrofluid over a stretching sheet respectively and highly nonlinear ODEs were solved by shooting method along with RK fourth order scheme. Abraham and Titus (2011) suggested that the influence of magneto-thermo mechanical interaction reduces with the impact of heat source/sink which causes the reduction of flow and heat transport rate.

Neuringer and Rosensweig (1964) presented a model with the statement that the magnetic field vector H is acting parallel to the magnetization M and Anderson and Valnes (1998) also assumed that H and M are acting in the same direction. Analytical work regarding ferrofluid motion can be studied in reference article Shliomis (2004) and Muhammad *et al*. (2017) premeditated the heat transportation in the ferrofluid past a stretched surface with temperature variation. Chyuan (2006) analyzed the thermo-magnetic convection phenomenon in the ferrofluid.

The purpose of current work is to describe the interaction of ferrofluid and magnetic dipole over a stretched sheet.

Initially, Crane (1970) solved this problem for Newtonian fluid but later on researchers extended this work towards non Newtonian fluids (Gibanov *et al*., 2017; Anderson *et al*., 1992; Chiam, 1982). Andersson and Valnes (1998) expanded the professed problem of Crane (1970), taking into account the effects of magneto-hydrodynamic and magnetic dipole, in a dynamical problem of non conducting viscous ferrofluid flow over a stretching sheet. The object of the present study is to scrutinize the magnetic structure of fluid flow as well as heat transport past an extending sheet by taking the effects of ferro-hydrodynamic and magnetic field along with other parameters. Our proposed method (SOR) is used for the first time to solve the flow problem involving magnetic dipole and ferrofluids. The impacts of the concerned parameters, involved in the flow model governing equations, will be illustrated graphically.

Description of physical model. Let us assume two dimensional steady flow past a stretching sheet and assume that flow is viscous, laminar and incompressible. The static B_0 (magnetic field) is normal to V (velocity field). An extending surface (sheet) causes the motion of the immobile fluid and the rate at which the surface is being extended is proportional to a length from a located position (x=0). The extending surface is placed at T_w (fixed temperature) below T_c (Curie temperature) as appeared in Fig. 1. The dipole produces a magnetic force of enough strength to concentrate the ferrofluid. In addition, the centre of dipole is located at y-axis away from x-axis at distance 'a' and whose magnetic field is specified in the positive x-direction.

Where all abbreviation are describe in below:

u=Velocity component along the sheet; v=Velocity component normal to the sheet; f=Dimensionless stream function; c=Constant; Pr=Prandtl number; M=Magnetic parameter; K=Constant; α=Coordinate along the sheet; y=Coordinate normal to the sheet; a=Dimensionless distance; σ_e=Electric conductivity; p=Pressure; λ=Viscous dissipation parameter; ρ=Density; β=Ferro hydrodynamic parameter; ε=Dimensionless Curie temperature; C_p=Specific heat; U=Free stream velocity of fluid; μ_0=Magnetic permeability; μ=Dynamic viscosity; T=Temperature; H=Applied magnetic field; k_0=Thermal conductivity; M=Magnetization; m=Stretching of sheet constant; η=Dimensionless coordinate

Under these assumptions and following Rosensweig (1985), the governing euations might be composed as:

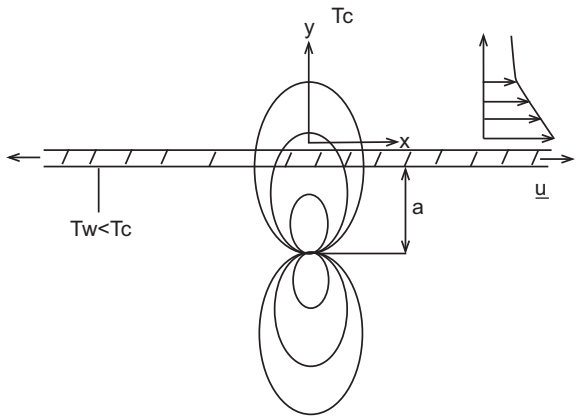

Fig. 1. Flow configuration model.

$$\partial v/\partial y+\partial u/\partial x=0 \quad \text{.....(1)}$$

$$u(\partial u/\partial x)+v(\partial u/\partial y)=-(1/\delta)(\partial p/\partial x)+(\mu_0/\rho)M(\partial H/\partial x)+(\mu/\rho)(\partial^2 u/\partial y_2)+\{(\sigma_e B_0^2)/(\rho)\}(U-u) \quad \text{.....(2)}$$

$$\rho C_p\{v(\partial T/\partial y)+u(\partial T/\partial x)\}+\mu_0 T(\partial M/\partial T)\{v(\partial H/\partial y)+u(\partial H/\partial x)\}=k_0(\partial^2 T/\partial y^2) \quad \text{.....(3)}$$

whereas velocity components (u and v) are specified along x and y-axis and σ_e is the electric conductivity; p denotes the pressure; ρ is the density; C_p is the specific heat; U is the free stream velocity of fluid; μ_0 is the magnetic permeability; μ is dynamic viscosity; T is temperature; H is applied magnetic field; k_0 is thermal conductivity and M is magnetization.

The appropriate boundary conditions (BCs) at y=0 where:

$$u(x,0)=cx,\ T(x,0)=T_w,\ v(x,0)=0 \quad \text{.....(4)}$$

whereas the BCs as $y\to\infty$

$$u(x,\infty)=0,\ p(x,\infty)=p_0-\rho a^2/2(x^2+y^2),\ T(x,\infty)=T_c \quad \text{.....(5)}$$

The applied magnetic field H affects the ferrofluid flow, whose magnetic scalar potential ϕ is defined as

$$\phi=\alpha/2\pi[x/\{x^2+(y+\alpha^2)\}^2] \quad \text{.....(6)}$$

And the components H_x and H_y corresponding to magnetic field H are given as

$$H_x=-(\partial\phi/\partial x)=\gamma/2\pi[\{x^2-(y+a)^2\}/\{x^2+(y+a^2)\}^2] \quad \text{.....(7)}$$

$H_y=-(\partial\phi/\partial y)=\gamma/2\pi[\{2x(y+a)\}/\{x^2+(y+a^2)\}^2]$.....(8)

Since the magnitude of ΔH is proportional to the body force so from $H=[(\partial\phi/\partial x)^2+(\partial\phi/\partial y)^2]^{1/2}$ we obtain (after expanding in powers of x and retaining terms up to order x^2):

$\partial H/\partial x=-(\gamma/2\pi)\{2x/(y+a)^4\}$ .....(9)

$\partial H/\partial x=\gamma/2\pi[-\{2/(y+a)^3\}+\{4x^2/(y+a)^5\}]$.....(10)

Spatially varying field must exist in the ferrohydrodynamic interaction (Neuringer and Rosensweig, 1964). Ferrofluid is saturated by applying the strong magnetic field H. The change in temperature as well as magnetization M is calculated from $M=K(T_c-T)$ with the assumption that curie temperature T_c is different from temperature T. Where T_c indicates the Curie temperature and K describes the pyromagnetic coefficient as suggested by Neuringer (1966) and Amirat and Hamdache (2012).

Solution procedure. Now, we introduce the nondimensional coordinates

$\eta=\sqrt{(c/v)}\, y$, $\Psi=\sqrt{(cv)}\, x f(\eta)$,

$\theta(\xi,\eta)\equiv(T_c-T)/(T_c-T_w)=\theta_1(\eta)+\xi^2\theta_2(\eta)$,.....(11)

$p=p_0-(\rho a^2/2)(x^2-y^2)$

By using Ψ (stream function), u and v can be related as:

$u=cxf'(\eta)$, $v=-\sqrt{(cv)}\, f(\eta)$.....(12)

Where prime indicates $df/d\eta$ and equation (1) is identically satisfied for u and v given in (12), while equations (2) and (3) are altered into following ODEs:

$f'''+ff''-f'^2+M^2(1-f')+1-\{(2\beta\theta_1)/(\eta+\alpha)^4\}=0$ .....(13)

$\theta_1''+Prf\theta_1'+[\{2\lambda\beta(\theta_1-\varepsilon)f\}/(\eta+\alpha)^3]=0$.....(14)

$\theta_2''-Pr(2f'\theta_2-f\theta_2')+[(2\lambda\beta f\theta_2)/(\eta+\alpha)^3]-\lambda\beta(\theta_1-\varepsilon)[\{(2f')/(\eta+\alpha)^4\}+\{(4f)/(\eta+\alpha)^5\}]=0$.....(15)

Where equal coefficients of ξ and ξ^2 have been equated in equation (3). Now the analogous BCs (4) and (5) become:

$f=0$, $f'=m$, $\theta_1=1$, $\theta_2=1$ At $\eta=0$ .....(16)

$f'\to1$, $\theta_1\to0$, $\theta_2\to0$ As $\eta\to\infty$.....(17)

Here m is stretching of sheet parameter and the remaining six parameters appear explicitly in equations (13)-(15) are:

$M=\sqrt{\{(\sigma_e B_0^2)/(\rho a)\}}$ is the Magnetic parameter
$Pr=\mu c_p/k$ is the Prandtl number
$\beta=(\gamma/2\pi)\mu_0 K(T_c-T_w)\rho/\mu^2$ is the Ferrohydro dynamic parameter.....(18)
$\varepsilon=T_c/(T_c-T_w)$ is the Dimensionless curie temperature
$\lambda=c\mu^2/\rho k(T_c-T_w)$ is the Viscous dissipation parameter
$\alpha=(c/v)^{1/2}a$ is the Dimensionless distance

Numerical solution using successive over relaxation (SOR) method. So, as to decide the numerical access, a typical approach is to change over the equations (9)-(12) in an initial value problem. Subsequently, shooting method alongside Runge Kutta (RK) technique might be consolidated to tackle the first order differential equations. A genuine deficiency shows up, if the linear system of ODEs includes widely spread eigenvalues where RK technique doesn't function admirably. Specifically, RK technique endures a lot of trouble to find solution of a set of differential equations involving a fast and slow state dynamics. Similarly, shooting methodology is progressively powerful when the shooting interval is short and the numerical solution is exceptionally influenced by the length of the distance (shooting) interval. In some cases, the calculation gets unstable even for very accurate estimates of initial conditions. This attribute may be because of the certain reliance of the solution on unique (original) initial conditions. A finite difference approach may not experience the ill effects of these inadequacies. Along these lines prior work (Ahmad *et al*., 2020a, b, c, d & e; 2019) included a methodology dependent on finite difference based technique which is not the same as the typical shooting system.

Using the same idea, the nonlinear equations (13)-(15) have been solved by employing finite difference discretization. Some complications may be found in the numerical solution of the boundary value problems comprising boundary layer equations, if the outer boundary conditions are positioned at infinity. The greater estimation values of the independent variable may numerically approximate the infinity in the test

integration. But there is no idea or any general rule to estimate these values. Choosing a large estimation value for the independent variable may converge very slowly or diverge the solution. In the same way, very small value may not offer the appropriate accuracy in the trial integration. However, exploiting the SOR method one can overcome such type of difficulties. The SOR method is an eminent technique to determine the numerical approximations of nonlinear and fully coupled differential equations in no times.

To solve the nonlinear coupled equations (13)-(15) problem, construct numerical algorithm based on finite difference technique (Ahmad *et al*., 2020a, b, c, d & e). As prescribed by Chamkha (2000), to recede the order of equation (13) by modifying

$$q=f'=df/d\eta \quad \text{.....(19)}$$

so, that we may write the nonlinear equations (13)-(15) as:

$$q''+fq'-q^2+M^2(1-q)+1-\{(2\beta\theta_1)/(\eta+\alpha)^4\}=0 \quad \text{.....(20)}$$

$$\theta_1''+Pr\, f\,\theta_1'+\{2\lambda\beta(\theta_1-\varepsilon)f\}/(\eta+\alpha)^3=0 \quad \text{.....(21)}$$

$$\theta_2''-Pr(2q\theta_2-f\theta_2')+\{(2\lambda\beta f\theta_2)/(\eta+\alpha)^3\}-\lambda\beta(\theta_1-\varepsilon)[2q/(\eta+\alpha)^4+4f/(\eta+\alpha)^5]=0 \quad \text{.....(22)}$$

subject to the relevant BCs:

$$f(0)=0,\ q(0)=m,\ q(\infty)=1,\ \theta_1(0)=1,\ \theta_1(\infty)=0,\ \theta_2(0)=1,\ \theta_2(\infty)=0 \quad \text{.....(23)}$$

After using finite differences, equations (20)-(22) take the form:

$$q_1=1/A_1(B_1q_{i+1}+C_1q_{i-1}+D_1) \quad \text{.....(24)}$$

$$\theta_{1_i}=1/A_2(B_2\theta_{i+1}+C_2\theta_{i-1}+D_2) \quad \text{.....(25)}$$

$$\theta_{2_i}=1/A_3(B_3\theta_{i+1}+C_3\theta_{i-1}+D_3) \quad \text{.....(26)}$$

where:

$A_1=4+2h^2q_i+2h^2M$, $B_1=2+hf_i$, $C_1=2-hf_i$, $D_1=2h^2(M+1)-\{4h^2\beta\theta_1/(\eta+\alpha)^4\}$

$A_2=4-\{(4h^2\lambda\beta f_i)/(\eta+\alpha)^3\}$, $B_2=2+hPrf_i$, $C_2=2-hPrf_i$, $D_2=-\{(4h^2\lambda\beta\varepsilon f_i)/(\eta+\alpha)^3\}$

$A_3=4+4h^2Prq_i+\{4h^2\lambda\beta f_i/(\eta+\alpha)^3\}$, $B_3=2+hPrf_i$, $C_3=2-hPrf_i$, $D_3=-2h^2\lambda\beta(\theta_1-\varepsilon)\{2q_i/(\eta+\alpha)^4+4f_i/(\eta+\alpha)^5\}$

Where, h embodies the grid length. SOR method is a well renowned scheme to attain the solutions of coupled differential equations with very quick convergence. Initially and almost all together Frankel (1950) and Young (1950) entrenched the theory of SOR. In the theory of SOR, it is worth pronouncing here that one seeks the value of the relaxation parameter (extrapolation factor) ω that accelerates the iteration procedure for which the SOR method converges. However, Kahan (1958) resolved this problem by suggesting the value of ω in the interval (0,2).

For an appropriate choice of the relaxation parameter $0<\omega<2$, the iterative process is initiated with some initiatory guessed values for the unknowns q, θ_1 and θ_2, where the kth iteration executes the following steps:

- By exploiting the SOR method, the succeeding approximations $q^{(k+1)}$, $\theta_1^{(k+1)}$ and $\theta_2^{(k+1)}$ are generated respectively for the solution of equations (24)-(26) subject to the last six conditions in (23).
- New guess $f^{(k+1)}$ for the solution of (24) is processed, subject to the first condition given in equation (23), by Simpson's rule which is then utilized in equation (24) to find q.
- For the convergence test $q^{(k+1)}$, $\theta_1^{(k+1)}$, $\theta_2^{(k+1)}$and $f^{(k+1)}$ are calculated along with $q^{(k)}$, $\theta_1^{(k)}$, $\theta_2^{(k)}$ and $f^{(k)}$.
- The iterative process is continued as far as:

$$\|q^{(k+1)}-q^{(k)}\|_{L_2}<TOL_{iter},\quad \|\theta_1^{(k+1)}-\theta_1^{(k)}\|_{L_2}<TOL_{iter},$$

$$\|\theta_2^{(k+1)}-\theta_2^{(k)}\|_{L_2}<TOL_{iter},\quad \|f^{(k+1)}-f^{(k)}\|_{L_2}<TOL_{iter},$$

For all the calculations performed here, the value of TOL_{iter} is fixed as 10^{-11}.

Results and Discussion

This section visualizes the numerical outcomes through tables and graphs. The non linear equations (13)-(15) are numerically solved with the help of BCs (16) and (17) by employing SOR technique, as described in the book by Hildebrand (1978), for a variety of estimation values assigned to governing parameters. The step sizes as well as the edges (for boundary layers) are balanced such that the flow and temperature profiles show asymptotic demeanor for various scope of physical parameters. The values of three parameters are fixed (i.e. $\alpha=1$, $\lambda=0.01$, $\varepsilon=2$) in agreement with the values of

parameters assumed by Neuringer (1966). The value of stretching sheet parameter is taken as m=0.5 otherwise identified and values of the remaining parameters are specified in graphs. While observing the thermal distribution, it is examined that the thermal boundary layers become thin with the influence of Pr (Prandtl number) and the temperature profile falls down in the flow region with an icrease in the values of Pr. The same trend in the thermal distribution was observed by Bognar and Hriczo (2018) as shown in Fig. 2.

The wall heat transport parameter in non-dimensional form is given as:

$$\theta'(0)=\theta_1'(0)+\xi^2\theta_2'(0) \quad \text{.....(26)}$$

It is ostensible that the bio magnetic interaction parameter β substantially affects the flow field. On the other hand for β=0 (hydrodynamic case), the flow problem becomes decouple for the thermal energy problem. Thereby, as suggested by Tzirtzilakis and Tanoud (2003), it is more expedient and interesting to change the dimensionless parameter θ′(0) given in equation (26) by the ratio:

$$\theta'(0)=\frac{\theta_1'(0)}{\theta_1'(0)|_{\beta=0}} \quad \text{.....(27)}$$

This dimensionless ratio does not depend on ξ and expresses heat transport rate on the surface (sheet).

The values of f″(0) and θ′(0) increase with M while the impact of stretching sheet parameter m is to decline the shear stress and increase the heat transport rate as predicted in Table 1. It is obvious from Table 2 that the shear stress and heat transportation rate increase by increasing the values of dimensionless distance α whereas ferrohydro dynamic parameter β acts in an opposite way as compared to α in case of shear stress. Accomplished results on the ferrofluid flow by Neuringer (1966) designated that the decrease in the values of f″(0) is slightly non-linear by increasing β. In our case, ferrohydrodynamic parameter β acts in the same way for f″(0) as mentioned by Neuringer (1966). Besides, the heat transport rates increase with an increment in λ, Pr & ε respectively, as envisioned in Table 3. It has been come into noticed that the Nusselt numbers (representing heat transportation rates) are the increasing functions of $Pr=\mu c_p/k$ (Prandtl number), $\lambda=c\mu^2/\rho k(T_c-T_w)$ (viscous dissipation parameter) and $\varepsilon=T_c/(T_c-T_w)$ (dimensionless Curie temperature) whereas the shear stress f″(0) is decreasing function of ferrohydro-dynamic

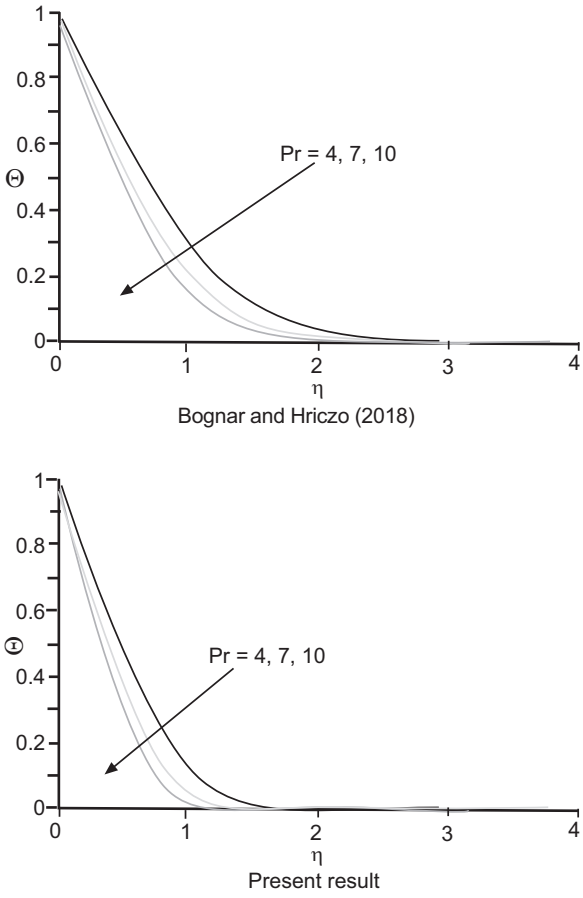

Fig. 2. Temperature profiles for various Pr with β=0.1 and m=0.

Table 1. Shear stress and heat transport rate for various M and m

M	f″(0)	θ′(0)	m	f″(0)	θ′(0)
0	0.1441	0.9682	0.0	2.0356	0.9684
2	0.4868	0.9764	0.2	1.5754	0.9748
4	0.7427	0.9807	0.4	1.0979	0.9798
6	0.9545	0.9835	0.6	0.6036	0.9837
8	1.1385	0.9855	0.8	0.0929	0.9868

Table 2. Shear stress and heat transport rate for various α and β

α	f″(0)	θ′(0)	β	f″(0)
0.20	-28.0387	0.1232	4	0.3692
0.22	-20.3245	0.3878	8	-0.6133
0.24	-15.2478	0.5470	12	-1.6347
0.26	-11.6823	0.6510	16	-2.7081
0.28	-9.0854	0.7234	20	-3.8565

Table 3. Heat transport rates for several λ, Pr and ε

λ	θ′(0)	Pr	θ′(0)	ε	θ′(0)
3	1.8947	1	0.9816	0	0.971306
6	3.3109	3	0.9838	5	1.066120
9	5.6902	5	0.9857	10	1.161176
12	10.2399	7	0.9872	15	1.256475
15	21.1413	10	0.9889	20	1.352016

parameter β. This study leads to the results that the shear stresses and heat transportation rates may be adjusted by appropriately selecting parametric values at the surface (sheet) to attain the required consequences in factual engineering applications of the present problem.

Figures 3 and 4 display the velocity f′(η) for a variety of estimation values of magnetic parameter M and stretching of sheet parameter m respectively, while the other parametric values are not changed (fixed). The velocity profiles f′(η) show an increasing trend across the boundary layer with M and m. One may conclude that the effect of both the parameters (M and m) is to enhance the flow velocities. Figures 5-7 demonstrate the influence of dimensionless distance α on flow and thermal velocities. As the values of α ascend, the velocity profile rises while the temperature profiles fall down. On the other hand, a reverse display can be seen for the ferrohydro dynamic parameter β as compared to α i.e. with an increment in β-values, the flow velocity depreciates and the temperature profiles rise up as shown in figures 8-10. These results indicate that the role of increasing α is to accelerate the flow velocity, while the ferrohydro dynamic parameter acts oppositely. From Figs. 11 and 12, we note that with escalating values of λ, the temperature profile $\theta_1(\eta)$ decreases whereas $\theta_2(\eta)$ increases. Figures 13 and 14 demonstrate the influence of Pr on the profiles $\theta_1(\eta)$ & $\theta_2(\eta)$. The temperature profiles fall with the effect of Prandtl number. Figures 15 and 16 predict that the temperature profile $\theta_1(\eta)$ decrease while $\theta_2(\eta)$ rise up by enlarging ε. It can be notified here that the increasing β-values cause the reduction in f′(η) and also tend to diminish the heat transportation rate at sheet. The coupling in the momentum as well as in the thermal energy equations is due to the presence of magnetic-dipole, which reduces the flow along the extending surface and decreases the heat transport rate as well. It is also notable that the impositions of the parameters λ, Pr & ε have exceeding influences on Nu_x.

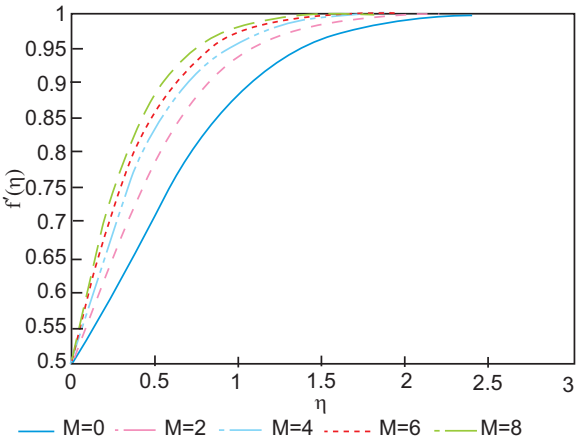

Fig. 3. Stream wise velocity f′(η) for β=2, Pr=7 and several M.

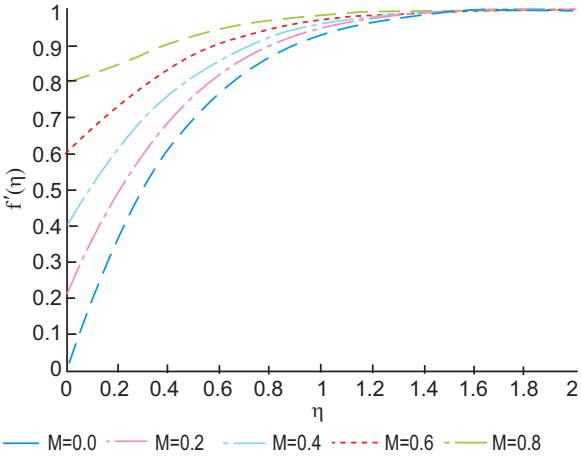

Fig. 4. Stream wise velocity f′(η) for β=2, Pr=7, M=5 and several m.

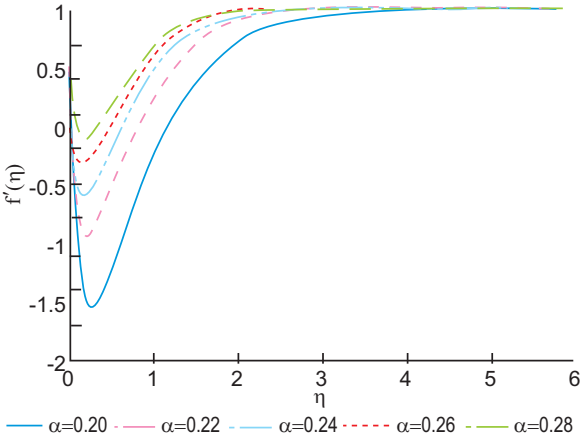

Fig. 5. Stream wise velocity f′(η) for β=0.5, M=2, Pr=0.7 and various α.

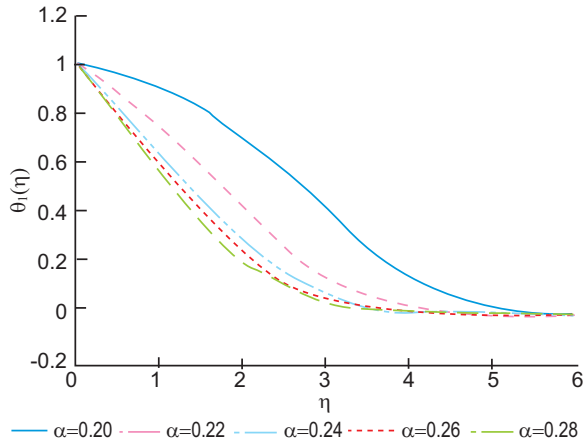

Fig. 6. Temperature profile $\theta_1(\eta)$ for β=0.5, M=2, Pr=0.7 and various α.

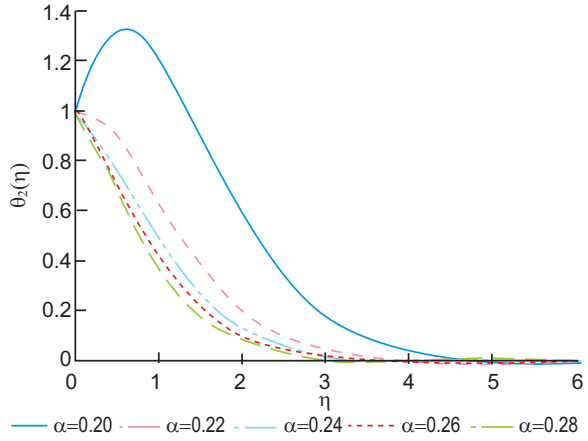

Fig. 7. Temperature profile $\theta_2(\eta)$ for β=0.5, Pr=0.7, M=2 and several α.

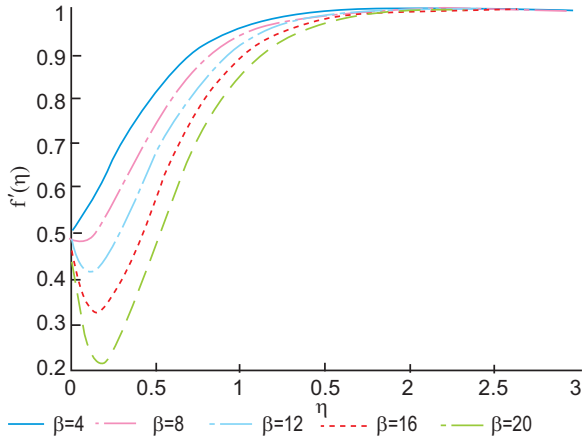

Fig. 8. Stream wise velocity $f'(\eta)$ for Pr=7, M=5 and several β.

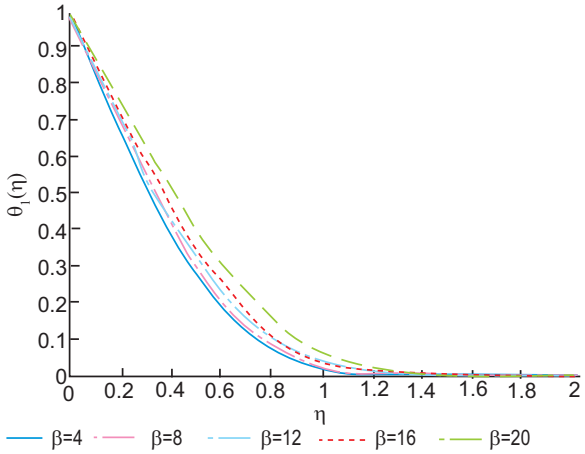

Fig. 9. Temperature profile $\theta_1(\eta)$ for Pr=7, M=5 and several β.

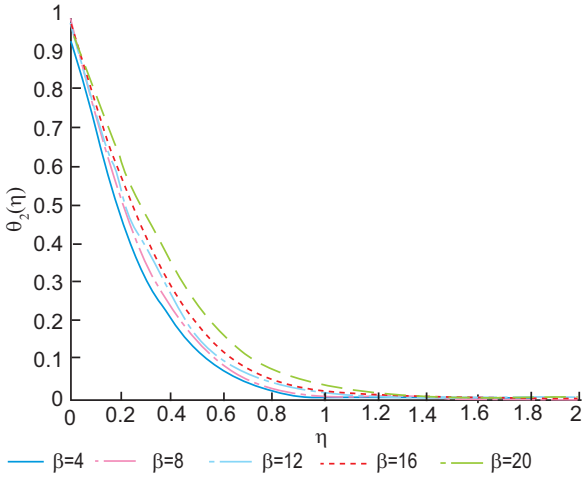

Fig. 10. Temperature profile $\theta_2(\eta)$ for Pr=7, M=5 and several β.

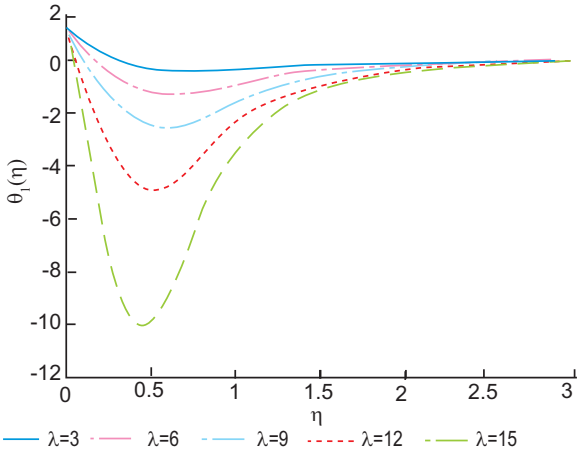

Fig. 11. Temperature profile $\theta_1(\eta)$ for β=2, Pr=7, M=5 and several λ.

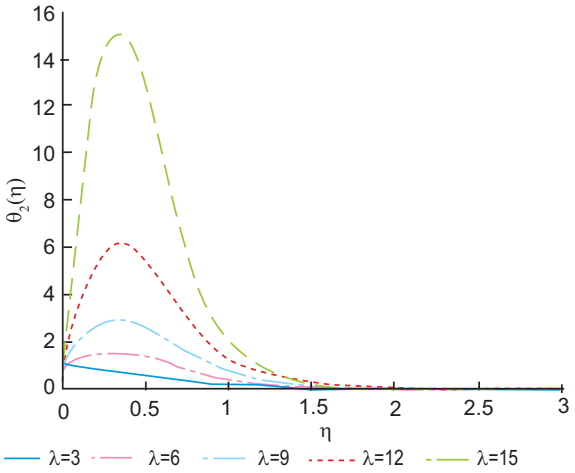

Fig. 12. Temperature profile $\theta_2(\eta)$ for $\beta=2$, Pr=7, M=5 and several λ.

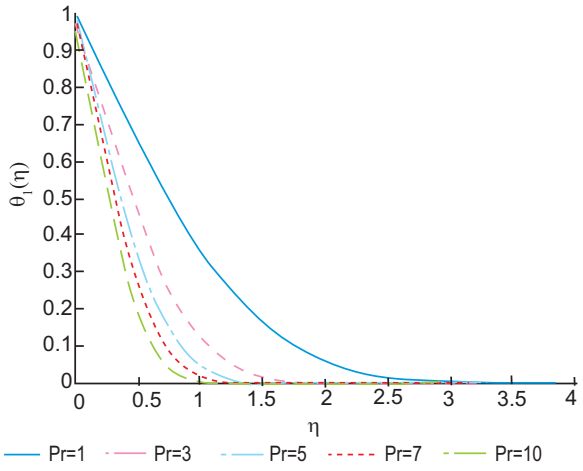

Fig. 13. Temperature profile $\theta_1(\eta)$ for $\beta=2$, M=5 and several Pr.

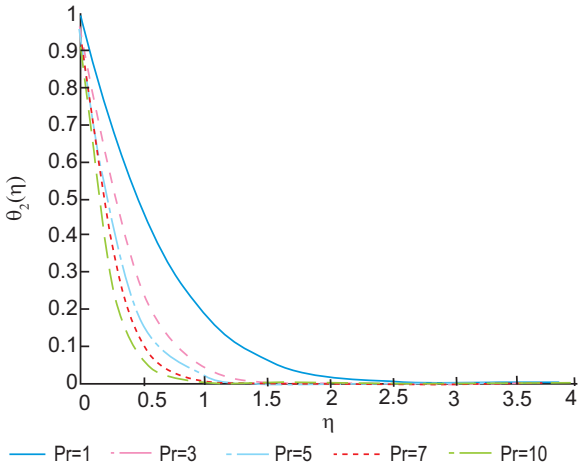

Fig. 14. Temperature profile $\theta_2(\eta)$ for $\beta=2$, M=5 and several Pr.

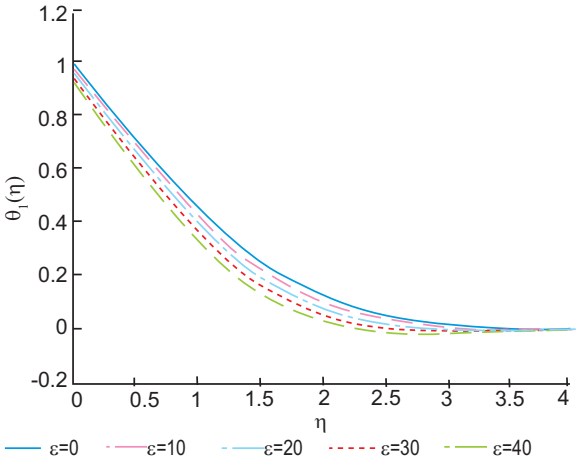

Fig. 15. Temperature profile $\theta_1(\eta)$ for $\beta=2$, Pr=0.7, m=1, M=2 and several ε.

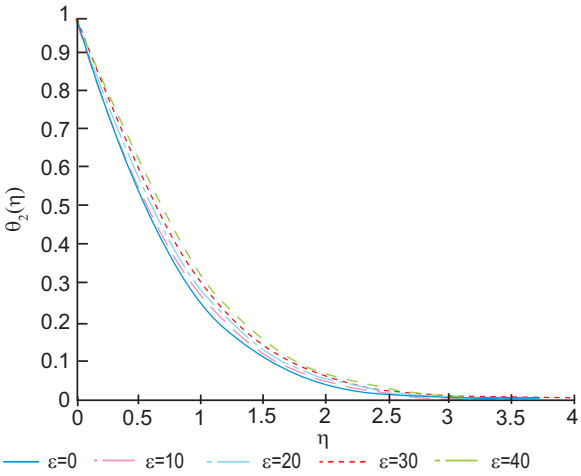

Fig. 16. Temperature profile $\theta_2(\eta)$ for $\beta=2$, Pr=0.7, m=1, M=2 and several ε.

Conclusion

This study reflects the impacts of magnetic parameter, stretching of sheet parameter, dimensionless distance, ferrohydrodynamic parameter, viscous dissipation parameter, Prandtl number and dimensionless Curie temperature on laminar, steady, two-dimensional and incompressible flow of ferrofluid with heat transport towards a stretching sheet. Non dimensional factors were exploited to transmute the governing PDEs into ordinary ones. The transmuted model subject to analogous BCs was then solved numerically with the help of SOR method along with finite difference discretization. The main achieved results are as follows:

- The curie temperature ε slightly affects the thermal distribution $\theta_2(\eta)$ while Viscous dissipation parameter λ marginally affects $\theta_2(\eta)$.
- Both the parameters, dimensionless distance α and the ferrohydro dynamic parameter β, act in an opposite way in case of velocity and thermal distribution.
- Enlarging values of the magnetic field parameter lead to enhance $f''(0)$ as well as $\theta'(0)$.
- The values of the heat transport rate $\theta'(0)$ increase with ascending values of λ, Pr & ε respectively.

Conflict of Interest. The authors declare that they have no conflict of interest.

References

Abbas, Z., Mushtaq, T., Shehzad, S.A., Rauf, A., Kumar, R. 2019. Slip flow of hydromagnetic micropolar nanofluid between two disks with characterization of porous medium. *Journal of the Brazilian Society of Mechanical Sciences and Engineering*, **41:** 465. https://doi.org/10.1007/s40430-019-1974-6

Abraham, A., Titus, L.S.R. 2011. Boundary layer flow of ferrofluid over a stretching sheet in the presence of heat source/sink. *Mapana Journal of Sciences*, **10:** 14-24. https://doi.org/10.12723/mjs.18.2.

Ahmad, S., Ashraf, M., Ali, K. 2020a. Heat and mass transfer flow of gyrotactic micro organisms and nano particles through a porous medium. *International Journal of Heat and Technology*, **38:** 395-402. https://doi.org/10.18280/ijht.380215

Ahmad, S., Ashraf, M., Ali, K. 2020b. Simulation of thermal radiation in a micropolar fluid flow through a porous medium between channel walls. *Journal of Thermal Analysis and Calorimetry*, **144:** 941-953. https://doi.org/10.1007/s10973-020-09542-w

Ahmad, S., Ashraf, M., Ali, K. 2020c. Micropolar fluid flow with heat generation through a porous medium. *Punjab University Journal of Mathematics*, **52:** 101-113.

Ahmad, S., Ashraf, M., Ali, K. 2020d. Nanofluid flow comprising gyrotactic microorganisms through a porous medium. *Journal of Applied Fluid Mechanics*, **13:** 1539-1549. DOI: 10.36884/jafm.13.05.31030

Ahmad, S., Ashraf, M., Ali, K. 2020e. Nanofluid flow comprising gyrotactic microbes through a porous medium - a numerical study. *Thermal Science*. https://doi.org/10.2298/TSCI190712332A

Ahmad, S., Ashraf, N., Ali, K. 2019. Numerical simulation of viscous dissipation in a micropolar fluid flow through a porous medium. *Journal of Applied Mechanics and Technical Physics*, **60:** 996-1004.

Alizadeh-Haghighi, E., Jafarmadar, S., Khalil Arya, S.H., Rezazadeh, G. 2017. Study of micropolar fluid flow inside a magneto-hydrodynamic micropump. *Journal of the Brazilian Society of Mechanical Sciences and Engineering*, **39:** 4955-4963.

Amirat, Y., Hamdache, K. 2012. Heat transfer in incompressible magnetic fluid. *Journal of Mathematical Fluid Mechanics*, **14:** 217-247.

Andersson, H.I., Valnes, O.A. 1998. Flow of a heated ferrofluid over a stretching sheet in the presence of a magnetic dipole. *Acta Mechanica*, **128:** 39-47. https://doi.org/10.1007/BF01463158.

Anderson, H.I., Bech, H., Dandapat, B.S. 1992. Magneto-hydrodynamic of a power law fluid over a stretching sheet. *International Journal of Nonlinear Mechanics*, **27:** 929-936. https://doi.org/10.1016/0020-7462(92)90045-9.

Bhatti, M.M., Abbas, T., Rashidi, M.M. 2016. Numerical study of entropy generation with nonlinear thermal radiation on magneto-hydrodynamics non Newtonian nanofluid through a porous shrinking Sheet. *Journal of Magnetics*, **21:** 468-475.

Bognar, G., Hriczo, K. 2018. Similarity transformation approach for a heated ferrofluid flow in the presence of magnetic field. *Electronic Journal of Qualitative Theory of Differential Equations*, **42:** 1-15. https:// doi.org/10.14232/ejqtde.2018.1.42.

Chamkha, A.J., Rashad, A.M., Alsabrey, A.I., Abdelrahman, Z.M.A., Nabwey, H.A. 2020. Impact of partial slip on magneto-ferrofluids mixed convection flow in enclosure. *Journal of Thermal Science and Engineering Applications*, **20:** 051002.

Chamkha, A.J., Issa, C.A. 2000. Effects of heat generation/absorption and thermophoresis on hydromagnetic flow with heat and mass transfer over a flat surface. *International Journal of Numerical Methods for Heat and Fluid Flow*, **10:** 432-449.

Chiam, T.C. 1982. Micropolar fluid flow over a stretching sheet. *Zeitschrift für Angewandte Mathematik und Mechanics*, **62:** 565-568. https://doi.org/10.1002/zamm.19820621010.

Chyuan, T.J. 2006. Analysis of combined thermal and magnetic convection ferro fluid flow in a cavity.

International Communications in Heat and Mass Transfer, **33:** 846-852. https://doi:10.1016/j.icheatmasstransfer.2006.02.001.

Crane, I.J. 1970. Flow past a stretching plate. *Zeitschrift für Angewandte Mathematik und Physik*, **21:** 645-647. http://dx.doi.org/10.1007/BF01587695.

EL-Kabeir, S.M.M., EL-Zahar, E.R., Modather, M., Gorla, R.S.R., Rashad, A.M. 2019. Unsteady MHD slip flow of a ferrofluid over an impulsively stretched vertical surface. *AIP Advances*, **9:** 045112. doi: 10.1063/1.5088610

El-Zahar, E.R., Rashad, A.M., Seddek, L.F. 2019. The impact of sinusoidal surface temperature on the natural convective flow of a ferrofluid along a vertical plate. *Mathematics*, **7:** 1014. doi:10.3390/math7111014

Eringen, A.C., Cemal, M., Gerard, A. 1990. *Electro-dynamics of Continua II: Fluids and Complex Media*. New York, Springer.

Frankel, S.P. 1950. Convergence rates of iterative treatments of partial differential equations. *Mathematical Tables and Other Aids to Computation*, **4:** 65-75.

Gangadhar, K., Narayana, K.L., Kumar, S.P., Bangalore, R.K. 2017. MHD micropolar fluid flow over a stretching permeable sheet in the presence of thermal radiation and thermal slip flow: a numerical study. *IOP Conference Series: Material Science and Engineering*, **263:** 062010. DOI: 10.1088/1757-899X/263/6/062010

Ghadikolaei, S.S., Hosseinzadeh, K., Yassari, M., Sadeghi, H., Ganji, D.D. 2018. Analytical and numerical solution of non Newtonian second grade fluid flow on a stretching sheet. *Thermal Science and Engineering Progress*, **5:** 309-316.

Gibanov, N.S., Sheremet, M., Oztop, H.F., Abu-Hamdeh, N.H. 2017. Effect of uniform inclined magnetic field on mixed convection in a liddriven cavity having a horizontal porous layer saturated with a ferrofluid. *International Journal of Heat and Mass Transfer*, **114:** 1086-1097. https://doi:10.1016/j.ijheatmasstransfer.2017.07.001.

Hildebrand, F.B. 1978. *Introduction to Numerical Analysis*. Tata McGraw-Hill Publishing Company, New Delhi, India.

Kahan, W. 1958. Gauss-Seidel Methods of Solving Large Systems of Linear Equations. *Doctoral Thesis*, University of Toronto, Toronto, Canada.

Muhammad, N., Nadeem, S., Haq, R. 2017. Heat transport phenomenon in the ferro-magnetic fluid over a stretching sheet with thermal stratification. *Results in Physics*, **7:** 854-861. https://doi.org/10.1016/j.rinp.2016.12.027.

Nabwey, H.A., Khan, W.A., Rashad, A.M. 2020. Lie group analysis of unsteady flow of kerosene/cobalt ferrofluid past a radiated stretching surface with Navier slip and convective heating. *Mathematics*, **8:** 826. doi:10.3390/math8050826

Neuringer, J.L. 1966. Some viscous flows of a saturated ferrofluid under the combined influence of thermal and magnetic field gradients. *International Journal of Nonlinear Mechanics*, **1:** 123-127. https://doi.org/10.1016/0020-7462(66)90025-4.

Neuringer, J.L., Rosensweig, R.E. 1964. Ferrohydro dynamics. *Physics of Fluids*, **7:** 1927-1937.

Papell, S.S. 1963. Low Viscosity Magnetic Fluid obtained by Colloidal Suspension of Magnetic Particles. *U.S. Patent* 3,215,572A, 9th October, 1963. doi: 19700030808.

Perez, L.M., Bragard, J., Diaz, P., Mancini, H.L., Laroze, D., Pleiner, H. 2017. Magneto viscous effect on thermal convection thresholds in an oldroyd magnetic fluid. *Journal of Magnetism and Magnetic Materials*, **444:** 432-438. https://doi.org/10.1016/j.jmmm.2017.07.052

Rashad, A.M. 2017. Impact of thermal radiation on MHD slip flow of a ferrofluid over a non isothermal wedge. *Journal of Magnetism and Magnetic Materials*, **422:** 25-31.

Rauf, A., Shehzad, S.A., Abbas, Z., Hayat, T. 2019. Unsteady three dimensional MHD flow of the micropolar fluid over an oscillatory disk with Cattaneo-Christov double diffusion. *Applied Mathematics and Mechanics-English Edition*, **40:** 1471-1486.

Rosensweig, R.E. 1985. Ferrohydro-dynamics. Dover Publications, Mineola, New York, USA.

Shamshuddin, M.D., Thumma, T. 2019. Numerical study of a dissipative micropolar fluid flow past an inclined porous plate with heat source/sink. *Propulsion and Power Research*, **8:** 56-68.

Shliomis, M. 2004. Comment on ferrofluids as thermal ratchets. *Physical Review Letter*, **92:** 188901. https://doi.org/10.1103/PhysRevLett.92.188901.

Tangthieng, C., Finlayson, B.A., Maulbetsch, J., Cader, T. 1999. Heat transfer enhancement in ferrofluids subjected to steady magnetic fields. *Journal of Magnetism and Magnetic Materials*, **201:** 252-255. https://doi:10.1016/S0304-8853(99)00062-1.

Tzirtzilakis, E.E., Tanoudis, G.B. 2003. Numerical study

of biomagnetic fluid flow over a stretching sheet with heat transfer. *International Journal of Numerical Methods for Heat & Fluid Flow*, **13:** 830-848. DOI 10.1108/09615530310502055.

Yacob, N.A., Ishak, A. 2012. Micropolar fluid flow over a shrinking sheet. *Meccanica*, **47:** 293-299. https://doi.org/10.1007/s11012-011-9439-8

Young, D.M. 1950. Iterative Methods for Solving Partial Differential Equations of Elliptic Type. *Doctoral Thesis*, Harvard University Cambridge, MA.

Zeeshan, A., Majeed, A., Ellahi, R. 2016. Effect of magnetic dipole on viscous ferro-fluid past a stretching surface with thermal radiation. *Journal of Molecular Liquids*, **215:** 549-554. https://doi.org/10. 1016/j.molliq.2015.12.110.